Partitioning between atmospheric deposition and canopy microbial nitrification into throughfall nitrate fluxes in a Mediterranean forest

(Article begins on next page)

27 April 2024

This is the final peer-reviewed accepted manuscript of:

Partitioning between atmospheric deposition and canopy microbial nitrification into throughfall nitrate fluxes in a Mediterranean forest

Rossella Guerrieri, Lucas Lecha, Stefania Mattana, Joan Cáliz, Emilio O. Casamayor, Anna Barceló, Greg Michalski, Josep Peñuelas, Anna Avila, Maurizio Mencuccini

The final published version is available online at:

Terms of use:

Journal of Ecology

DR ROSSELLA GUERRIERI (Orcid ID : 0000-0001-5247-0432)

MISS EMILIO O. CASAMAYOR (Orcid ID : 0000-0001-7074-3318)

Article type   : Research Article

Handling Editor: Ana Pineda

Partitioning between atmospheric deposition and canopy microbial nitrification into throughfall nitrate fluxes in a Mediterranean forest

Rossella Guerrieri[1*], Lucas Lecha[1], Stefania Mattana[1], Joan Cáliz[2], Emilio O. Casamayor[2], Anna Barceló[3], Greg Michalski[4], Josep Peñuelas[1,5], Anna Avila[1], Maurizio Mencuccini[1,6]

[1] *CREAF, E08193 Bellaterra (Cerdanyola del Vallès), Catalonia, Spain*

[2]*Integrative Freshwater Ecology Group, Centre of Advanced Studies of Blanes, CEAB-CSIC, Spanish Council for Scientific Research), E-17300 Blanes (Spain)*

[3]*Servei de Genòmica i Bioinformàtica, IBB-Parc de Recerca UAB - Mòdul B, Universitat Autònoma de Barcelona, 08193 Bellaterra, Barcelona (Spain)*

[4]*Department of Earth, Atmospheric, and Planetary Sciences, Purdue University, 550 Stadium Mell Drive, West Lafayette, IN 47907 (USA)*

[5] *CSIC, Global Ecology Unit CREAF-CSIC-UAB, 08193 Bellaterra, Catalonia, Spain*

[6] *ICREA, Pg. Lluís Companys 23, 08010 Barcelona (Spain)*

* Corresponding author

Rossella Guerrieri (rossellaguerrieri@gmail.com)

Words count: 9634 (including authors' contribution, acknowledgment, table and figures legend.

Abstract: 308

Figures: 7

Table: 1

Abstract

1. Microbial activity plays a central role in nitrogen (N) cycling, with effects on forest productivity. Though N bio-transformations, such as nitrification, are known to occur in the soil, here we investigate whether nitrifiers are present in tree canopies and actively process atmospheric N.

2. This study was conducted in a Mediterranean holm oak (*Quercus ilex* L.) forest in Spain during the transition from hot dry summer to cool wet winter. We quantified NH_4^+—N and NO_3^-—N fluxes for rainfall (RF) and throughfall (TF) and used $\delta^{15}N$, $\delta^{18}O$, and $\Delta^{17}O$ to elucidate sources of NO_3^-. Finally, we characterized microbial communities and abundance of nitrifiers on foliage, RF and TF water through metabarcoding and quantitative Polymerase Chain Reaction, respectively.

3. NO_3—N fluxes at the site were larger in TF than RF, suggesting a contribution from dry deposition, as also supported by $\delta^{15}N$ and $\delta^{18}O$. However, $\Delta^{17}O$ indicated that about 20% of NO_3^- in TF derived from canopies nitrification in August, after a severe drought, with a lower proportion in September ($\approx 8\%$). This seasonal partitioning between biologically and atmospherically derived NO_3^- coincided with a decreasing trend of the abundance of archaeal nitrifiers. Tree canopies and TF had more diverse microbial communities than RF. Yet, RF showed higher variability in microbial composition, likely associated to the origin of air masses.

4. *Synthesis.* Atmospheric N deposition is significantly altered after passing through tree canopies. While nitrification has been proposed as one of the mechanisms responsible for these changes, very few studies directly investigate its occurrence. Here, we showed that nitrification by epiphytic leaf microbes contributed to increasing NO_3 in TF and that nitrifiers' activity was reduced going from the dry and hot summer to the cool winter.

Overall, these results highlight the power of coupling microbial community analysis, functional gene amplification and stable isotope approaches to examine ecosystem-scale processes.

Key words: ammonia-oxidizing bacteria, ammonia-oxidizing archaea, canopy nitrification, Mediterranean forest, metabarcoding, nitrate fluxes, stable isotopes, throughfall.

1. Introduction

Atmospheric concentrations of reactive nitrogen (N) substantially increased over the last century (Erisman *et al.*, 2011), due to burning of biomass and fossil fuels by vehicles, power plants and industries (i.e., NO_y = NO, NO_2 and NO_3) and the intensive use of fertilizers and livestock for food production (i.e., NH_x). These reactive N compounds, however, do not remain in the atmosphere but are deposited onto terrestrial and aquatic ecosystems as N deposition (N_{dep}), thus altering global N cycling (Galloway & Cowling, 2003). The input of N to forests from the atmosphere can lead to a cascade of positive (e.g., increasing carbon (C) sequestration in N-limited forests, Magnani *et al.*, 2007) and negative (e.g., loss of biodiversity, Dise *et al.*, 2011) effects, which eventually shift the balance between N accumulation and loss (Galloway & Cowling, 2003). The ultimate fate of the atmospheric N deposited onto forest ecosystems, though, is not fully understood.

Many studies, mostly based on soil-manipulation experiments, have suggested that soils are the main sink of atmospheric N_{dep} (Nadelhoffer *et al.*, 1999) and high inputs of N from the atmosphere affect soil biogeochemical processes (Reay *et al.*, 2010). However, monitoring the main inorganic N compounds (NH_4^+, NO_3^-, and dissolved organic N) in bulk precipitation (often indicated as rainfall in N_{dep} studies, hereafter referred to as RF) and in water collected underneath tree canopies, i.e., throughfall (TF), has shown that N_{dep} is substantially altered along its path through the canopy. Increases in N fluxes in TF relative to RF, particularly in forests receiving high N_{dep}, have been commonly attributed to leaching and washing of dry N_{dep} from the canopies by precipitation (e.g., Ferretti *et al.*, 2014, Vanguelova *et al.*, 2010, Griffith *et al.*, 2010), though this approach may underestimate total N_{dep} because tree canopies can retain part of the atmospheric N (e.g., Templer *et al.*, 2015). Lower N fluxes in TF than RF, however, have also been reported and have been considered an indication of retention by tree canopies and associated

epiphytes (e.g., Lindberg *et al.* 1986; Mustajärvi *et al.*, 2008; Dail *et al.* 2009; Ponette-González *et al.,* 2010; Woods *et al.* 2012; Fenn *et al.* 2013; Houle *et al.*, 2015) and of direct foliar uptake (e.g., Sparks 2009; Adriaenssens *et al.* 2012). A more mechanistic explanation of the differences between TF and RF for N fluxes is included in the canopy budget model (CBM), an approach commonly used to better estimate dry deposition. This model is based on balancing ion exchanges between canopies and the solutions passing through them, so that the uptake of NH_4^+ is accompanied by the leaching of K^+, Ca^+, or Mg^+ (Draaijers *et al.* 1996). Further developments of the CBM include canopy NO_3^- uptake as a proportion of NH_4^+ uptake (e.g., Adriaenssens *et al.*, 2013). This approach nevertheless assumes that tree canopies are passive receptors of atmospheric N (i.e. only uptake is considered) and that no biological transformation occurs.

Many studies since the early 1950s have demonstrated that forest canopies represent an important habitat (the phyllosphere) for microbial communities, which include bacteria, fungi, and yeasts (Andrew & Harris, 2000; Lindow & Brandl, 2003; Lambais *et al.* 2006; Delmotte *et al.*, 2009; Vacher *et al.*, 2016). The advent of next-generation sequencing (NGS) technologies (Shokralla *et al.* 2002), also known as high-throughput sequencing, has helped to identify the high diversity of bacterial communities in the phyllosphere and the major taxonomic species, although studies are still limited (Kembel *et al.*, 2014; Laforest-Lapointe *et al.*, 2016). Whether or not bacteria in the phyllosphere play a role in nutrient cycling, particularly N, is not well studied. The presence of N-fixing microbes in tree canopies has previously been reported in Mediterranean (e.g., Rico *et al.,* 2014) and boreal forests (Moyes *et al.*, 2016). Plants can use N derived from N fixation by endophytic N-fixing bacteria (Moyes *et al.*, 2016), but N fixation may well not be the only N transformation that occurs in tree canopies. Nitrifying bacteria and Archaea have been detected on spruce needles in a forest in Germany exposed to high N_{dep} (Papen *et al.,* 2002) and on foliar surfaces of *Cryptomeria japonica* (Watanabe *et al.*, 2016), by determining the number of cells of chemolithoautotrophic nitrifiers and the number of copies of the archaeal *amoA* gene, respectively.

While genetic approaches allow measuring the abundance of nitrifying species in the phyllosphere, they cannot track their activity. This can be accomplished instead using stable oxygen and nitrogen isotope ratios in NH_4^+ and NO_3^- of RF and TF. More ^{15}N-depleted NO_3^- found in TF than RF of a Norway spruce forest in central Europe (Sah & Brumme, 2003), a montane rainforest in Ecuador (Schwarz *et al.,* 2011), and Scots pine under high N_{dep} in the UK

(Guerrieri *et al.*, 2015) suggested nitrification occurred in the canopy, since nitrification of NH_4^+ leads to the production of ^{15}N-depleted NO_3^-, while residual NH_4^+ becomes more enriched in ^{15}N (Högberg, 1997). The measurement of $\delta^{17}O$ and $\delta^{18}O$ is a more robust approach to discriminate between atmospheric and biological transformations as sources of NO_3^-. Mass-dependent isotope fractionation leads to a consistent relationship between $\delta^{17}O$ and $\delta^{18}O$, i.e. $\delta^{17}O = 0.52 \cdot \delta^{18}O$ (Matsuhisa *et al.*, 1978; Miller, 2002; Young *et al.*, 2002). Mass-independent fractionations however, are observed for ozone-mediated NO_3^- formation in the atmosphere (Michalski *et al.*, 2002), which cause an equal enrichment in ^{18}O and ^{17}O. This 'excess' ^{17}O in NO_3^- is quantified by $\Delta^{17}O = \delta^{17}O - 0.52 \delta^{18}O$. The $\Delta^{17}O$ clearly provides a more robust estimate of the source of NO_3^- (Michalski *et al.*, 2003; Michalski *et al.*, 2012). Ozone-derived NO_3 has $\Delta^{17}O > 0$, but mass-dependent processes, such as microbial nitrification, produce NO_3^- with $\Delta^{17}O = 0$. Using a mass-balance approach based on the $\Delta^{17}O$ values for NO_3^- in RF and TF has uniquely demonstrated that a large fraction of the NO_3^- in TF can derive from nitrification in tree canopies, between 17 and 59% for Scots pine and beech forest under high N_{dep}, respectively (Guerrieri *et al.*, 2015). All these studies, though limited (compared to studies of soil nitrification), provide important evidence that canopies are not just passive filters of atmospheric N. Resolving the fate of deposited N when interacting with tree canopies is crucial for estimating its impact on forest N cycling.

We investigated the occurrence of nitrification in tree canopies and its contribution to TF fluxes in a Mediterranean holm oak forest. Specific goals were to: 1) quantify NO_3-N/NH_4-N fluxes in RF and TF during the transition from summer to winter, 2) characterise microbial communities in RF, TF and foliage, 3) determine whether microbial species and genes involved in nitrification in the canopy (bacterial and archaeal *amoA*) could be detected and their presence quantified, and 4) estimate the proportions of biologically and atmospherically derived NO_3^- in the canopy. We combined independent but complementary approaches, including chemical (NH_4^+ and NO_3^- concentrations in RF and TF), genetic (16S rRNA gene metabarcoding and gene-specific quantitative PCR (qPCR)), and isotopic ($\delta^{15}N$, $\delta^{18}O$, and $\delta^{17}O$ in NO_3^-) analyses.

2. Materials and Methods
2.1 Site description

The study site was in a *Quercus ilex* L. (holm oak) forest at La Castanya located in the Montseny Mountains in Spain (41°46′N, 2°21′E; 700 m a.s.l.), 40 km N-NE of Barcelona (Table 1) and 27 km from the Mediterranean Sea. The area has a meso-Mediterranean sub-humid climate with high inter-annual and seasonal variability in precipitation, which is lowest in summer and tends to be highest in spring and autumn (Aguillaume *et al.*, 2017). This site is topographically sheltered, to some extent, from the transport of air pollution from the Barcelona urban area. Diurnal sea-land breezes in summer, however, transport pollution from the coast and lowland plains to the upper Montseny slopes (Pérez *et al.*, 2008).

2.2 Water and foliar sample collection and filtration

To document the seasonal transition from hot dry summer to cool humid winter, we planned to collect water samples weekly from June to December 2016. However, due to prolonged drought in 2016, the first sampling was carried out in August. The number of sampling dates depended on the precipitation events and it was as follows: n=2 in August, November and December, and n=3 in September and October, and the total volume of water collected for each sample type is shown in the Figure S1. Wet deposition (RF) was collected in a G78-1001 wet-only deposition collector (ESM Andersen instruments, Erlangen Germany) in a clearing located at less than 500 m from the forest. The lid of the collector automatically opened at the start of rain and closed 10-15 min after the rain ended to avoid collecting ions from dry deposition. Ten TF collectors were randomly situated in a 30×30 m^2 plot within the investigated holm-oak forest, at 1.5 m off the ground.

These collectors consisted of an ISO-standardised funnel (Norwegian Institute for Air Research, NILU) with a 314-cm^2 horizontal interception surface connected to a 2-L polypropylene bottle. A mesh grid was placed in the funnel neck to prevent leaves and other material from entering the bottle. The upper edge of the funnel was equipped with an external ring to prevent contamination from bird droppings. All water samples were transported to the laboratory on the same day of collection, which normally occurred within 1-2 days after the precipitation event. Sixty millilitres of the total water collected on a given date were filtered with 0.45 μm pore size acetate cellulose membrane filters and frozen for NO_3^- and NH_4^+ quantification. The remainders of the RF and TF samples were proportionally combined to produce a composite monthly sample. We obtained between 0.25 L (in August) and 2 L (for the other months) of water for both RF and TF. Samples were stored at 4 °C in the dark until filtering within a month from collection for the subsequent determination of isotopic values in NO_3^-.

Four holm oak trees were selected next to the TF collectors for characterising the epiphytic microbial communities in the phyllosphere. Diameter at breast height and height of the selected trees were in the range of 15-18 cm and 7-9 m, respectively. Two branches at two canopy positions (top and intermediate/bottom) were sampled from each tree in November 2016. Each branch was then placed in a sterile plastic bag, labelled, and stored in situ in an insulated box with dry ice. The branches were then stored in the laboratory at - 20 °C.

2.3. Quantification of N fluxes

The RF and TF water samples described above were used to determine NO_3^- and NH_4^+ concentrations by ion chromatography (Dionex S-100 and Dionex ICS-1100, USA). Analytical quality was routinely checked with the ratio of the sum of cations to the sum of anions and the ratio of theoretical to measured conductivity (for both, ideally 1.00; admitting a 20% allowance) as described in Avila (1996). We calculated monthly deposition fluxes of NO_3-N and NH_4-N for RF by multiplying the mean monthly concentration of each ion in the RF samples (µEq/L, shown in Figure S2) by the monthly rainfall measured by a Hellman standard rain gauge (L/m^2) at the site. As for TF fluxes, we multiplied the mean monthly concentration (average of the 10 TF collectors) of each ion (in µEq/L) by the mean monthly TF volume (in L/m^2) averaged from the 10 TF collectors located in the holm oak plot. Thus, for TF, the monthly sample averaged both the temporal (weekly into monthly fluxes) and spatial (10 TF replicates) variability. N fluxes were then expressed in kg ha^{-1} month^{-1}.

2.4 Sample preparation for genetic analysis

Phyllosphere. To obtain epiphytic microbial DNA, between 6 and 7 grams of leaves were randomly collected from each of the two branches sampled per tree and placed in sterile 50-mL centrifuge tubes. Thirty-five millilitres of 1:50 diluted Redford buffer wash solution (1 M Tris·HCl, 0.5 M Na EDTA, and 1.2% CTAB; Kembel et al., 2014) were added to the tube, which was then agitated for 5 min. The washing solution was transferred to another sterile tube and centrifuged for 30 min at 3000 g. The pellet was transferred to 2-mL MO BIO PowerSoil bead-beating tubes for DNA extraction.

Water samples. To collect microorganisms, water samples (RF and TF) were filtered through 0.22-µm mixed cellulose membrane sterilized filters (S-Pak™ Membranes, Merck KGaA,

Darmstadt, Germany). The filters were then stored at -20 °C until genetic analysis. The RF samples collected each month were filtered using only one filter for each month. The TF samples for September, October, and December were pooled for every 3-4 collectors to provide three spatial replicates, which were filtered as described above. In contrast, the entire volumes collected for August and November were filtered to provide only one sample for each month. Filters for the genetic analyses were cut into pieces and transferred to 2-mL MO BIO PowerSoil bead-beating tubes. Microbial DNA was extracted from all samples using a MO BIO PowerSoil DNA isolation kit (MO BIO, Carlsbad, USA) following the manufacturer's instructions. DNA was quantified using a NanoDrop spectrophotometer (ThermoFisher, Wilmington, USA).

2.4.1 Functional gene quantification and DNA sequence processing

Aliquots of the microbial DNA from the foliar surfaces and water solution were used to i) prepare amplicon libraries for Illumina sequencing and ii) quantify through qPCR analysis the number of copies of the *amo*A gene, the functional gene involved in the first step of nitrification and present in ammonia-oxidizing bacteria (AOB) and ammonia-oxidizing Archaea (AOA). Details on both analyses are provided in the supplementary information.

The raw sequences of the 16S rRNA gene as obtained from the Illumina analyses were processed using the UPARSE pipeline (Edgar, 2013): i) reads (forward and reverse) were paired to obtain consensus sequences, ii) low-quality sequences were discarded based on the expected error filtering, set to 0.5, which is a more robust approach than using the quality score Q (Edgar & Flyvbjerg, 2015), and iii) sequences were dereplicated and clustered into operational taxonomic units (OTUs) at the 97% identity threshold, after excluding chimeric sequences and singletons. Taxonomic assignment used the RDP Classifier (Wang *et al.,* 2007) and the SILVA 123 database (Quast *et al.*, 2013). Chloroplast, mitochondrial, and unclassified sequences were excluded from further analyses. We obtained totals of 1350947 reads and 2661 OTUs, with 604 microbial genera identified across all samples. For each sample type, the mean (minimum-maximum) number of reads obtained were: RF =126660 (41399-193624); TF: 34328 (5830-95015); phyllosphere: 42504 (6353-95471). The original OTU table was rarefied (Figure S3) and set to a depth of 5000 sequences per sample (based on the minimum number of reads) to minimise biases for differences in sampling effort. The number of OTUs per sample ranged between 130 and 438 after rarefaction.

2.5 Stable isotope analyses and the mass-balance approach

The monthly composite RF and TF water samples were used for the measurements of the stable isotopes in NO_3^-. The samples were conveyed through an anion exchange resin (AG® 1-X8, analytical grade, 20-50 mesh, chloride form) to retain NO_3^-, which was then eluted from the resin using 20 mL of 1M KBr. These samples were then analysed by isotope-ratio mass spectrometry using the bacterial reduction and thermal decomposition methods (Casciotti *et al.*, 2002; Kaiser *et al.*, 2007). Briefly, NO_3^- in aqueous samples was bacterially reduced using a strain of *Pseudomonas aureofaciens* to convert aqueous phase NO_3^- to gas phase nitrous oxide (N_2O). Each vial was purged with helium, thus forcing the effluent through a nafion drier trap, removing most of the water vapour. A second trap containing Ascarite removed most of the CO_2 (99%) and residual water. Finally, any trace water was removed by a trap containing $MgClO_4$. The N_2O from the sample was thawed in a liquid-N trap and then transferred in a helium flow to a gold tube, where it was pyrolised at 850 °C to produce N_2 and O_2. The O_2 and N_2 were separated using a gas chromatograph with a 5-Å molecular sieve and analysed using a Finnigan Delta Plus Advantage continuous-flow isotope-ratio mass spectrometer (Thermo Fischer Scientific, Waltham, USA). The stable isotope ratios in our samples, $^{18}O/^{16}O$, $^{17}O/^{16}O$, and $^{15}N/^{14}N$, were expressed relative to those in international standards, i.e., Vienna Standard Mean Ocean Water (VSMOW) and atmospheric N_2 for the oxygen and nitrogen isotope ratios, respectively. The long-term analytical precision assessed on 12 replicates for a given run was about ± 0.2‰ for $\delta^{17}O$ and $\delta^{18}O$ and about ± 0.5‰ for $\delta^{15}N$. Stable isotope analyses were conducted at the Purdue Stable Isotope Laboratory (Purdue University, USA).

The fraction of NO_3^- from nitrification in the canopy relative to the fraction from atmospheric deposition was assessed using a mass-balance approach based on the $\Delta^{17}O$ values (Michalski *et al.*, 2003) measured in RF and TF, as described by Guerrieri *et al.*, (2015). Briefly, we started with the equation:

$$\Delta^{17}O_{TF} = f_{Bio}\left(\Delta^{17}O_{Bio}\right) + f_{Atm}\left(\Delta^{17}O_{Atm}\right) \qquad (1)$$

where $\Delta^{17}O_{TF}$ was derived from the measured $\delta^{17}O$ and $\delta^{18}O$ of NO_3^- in TF, $\Delta^{17}O_{Bio}$ and $\Delta^{17}O_{Atm}$ are the $\Delta^{17}O$ values of the biologically and atmospherically derived NO_3^-, respectively, and f_{Bio} and f_{Atm} are the two unknown NO_3^- flux fractions from the two sources, where:

$$f_{Bio} + f_{Atm} = 1 \qquad (2)$$

The f_{Atm} included the fractions of both the wet (f_{Wet}) and dry (f_{Dry}) NO_3^- depositions washed from

the canopy and the net of the fractions retained in the phyllosphere and/or taken up by leaves (f_U), i.e. $f_{Atm} = f_{Wet} + f_{dry} - f_U$. Assuming that $\Delta^{17}O_{Bio} = 0$ (Michalski *et al.*, 2003) and that $\Delta^{17}O$ of NO_3^- in RF represented both wet and dry N_{dep}, Eq. (1) can be reduced to:

$$f_{Atm} = \frac{\Delta^{17}O_{TF}}{\Delta^{17}O_{RF}} \qquad (3)$$

which can then be used in the equation 2 to obtain f_{Bio}.

2.6 Statistical analyses

OTU distance-based community analyses used Bray-Curtis dissimilarities after Hellinger standardisation (Legendre & Gallagher 2001) and were represented by non-metric multidimensional scaling (NMDS). OTU richness and Shannon diversity were calculated using standard formulae. A permutational analysis of variance (PERMANOVA, Anderson, 2001), as implemented in the R 'adonis' function, was used to test for differences across sample types (TF, RF, and foliar samples) and canopy positions (top and intermediate/bottom) for the phyllosphere, and time periods for TF. The multivariate homogeneity of group dispersions (variances in beta-diversity) was tested using the R 'permutest.betadisper' function across sample types. We identified significant associations between bacterial taxa and sample types using the Linear Discriminant Analysis Effect Size (LEfSe) algorithm (Segata *et al.*, 2011). This analysis identifies significant individual host-microbe associations at various taxonomic scales and evaluates the strength of associations amongst organisms from different groups (Segata *et al.*, 2011). We set the thresholds of the absolute value of the logarithmic linear discriminant analysis (LDA) score and the alpha value for the statistical test to the very restrictive values of 4 and 0.01, respectively, to minimize spurious associations. Spearman's correlation coefficient (R_s) was used to estimate the degree of correlation between the abundance of OTUs across sample types.

Functional gene, isotope and N flux data were checked for normality and homogeneity of variance by using Shapiro (and quantile-quantile plots) and Levene tests, respectively. Functional gene data were log-10 scaled, which improved the normality of data distribution. Differences in the number of copies of the archaeal *amoA* gene between canopy positions were assessed using an independent *t*-test. Linear regression was used to assess the changes in $\delta^{15}N$, $\delta^{18}O$ and $\Delta^{17}O$ and in the abundance of archaeal and bacterial *amoA* in the water samples over time. In this latter case,

since data were log-10 transformed, the slope from the linear regression analyses was expressed as percentage change as obtained from the following equation: ((exponential (slope) - 1) * 100). Differences in the means across months for both functional genes and the isotopic ratios of NO_3^- in TF were assessed by an analysis of variance (ANOVA), while the Tukey honest significant difference test was used for the multiple comparisons. Differences for $N—NO_3^-$ and $N—NH_4^+$ fluxes, within and across sample types, were assessed using a non-parametric Wilcoxon test (W), because the data did not meet the assumption of variance homogeneity, based on the Levene test. The level of significance of all statistical tests was set as $p \le 0.05$. Plots and statistical analyses were performed in R (R Core Team, 2016) using ggplot2 (Wickham, 2016), stats and Vegan packages (Dixon, 2003).

3. Results

3.1 Temporal changes in N fluxes

Total wet N_{dep} ($NH_4—N + NO_3—N$) at the site was 1.7 kg N ha^{-1} for August-December, based on RF fluxes, and 5 kg N ha^{-1} when TF fluxes were considered (Figure 1). The $NO_3—N$ fluxes were significantly higher than the $NH_4—N$ fluxes only for TF (Wilcoxon, W=0, $p< 0.05$), while no differences between the two N fluxes were observed in the case of RF. No significant differences were observed between RF and TF for $NH_4—N$ fluxes, whereas $NO_3—N$ fluxes were higher in TF than RF (W= 0, $p< 0.01$), with a mean difference of 0.59 ± 0.29 kg N ha^{-1} month^{-1}.

3.2. Structure and composition of bacterial communities in water and foliar samples

The structure of bacterial communities based on similarity metrics differed significantly across sample types (i.e., RF, TF, and leaves, PERMANOVA; $R^2= 0.58$ and $p< 0.001$) (Figure 2a). In addition, the multivariate homogeneity of groups' dispersions confirmed a higher beta-diversity in water versus foliar samples ($p< 0.001$) (Figure 2b). RF collected at different times had the highest dispersion amongst the bacterial communities, which, however, did not follow a summer to winter pattern. In contrast, TF communities for each sampling period tended to resemble each other (PERMANOVA; $R^2= 0.54$ and $p< 0.01$). Foliar samples had the most homogeneous epiphytic communities, which did not differ significantly between the top and intermediate/bottom positions in the canopy (PERMANOVA; $R^2= 0.23$ and $p> 0.05$). The alpha-diversity metrics OTU richness (unique OTUs) and Shannon's diversity index were lower in RF than TF and the foliar bacterial communities (ANOVA; $p < 0.001$) (Figure S4, panels a and b).

RF shared 65 and 45% of its OTUs with TF and the foliar samples, respectively, whereas 40% of the foliar OTUs were also found in TF. *Actinobacteria*, *Cytophagia*, and *Alphaproteobacteria* were amongst the most abundant classes in the phyllosphere (ca. 75%) (Figure 3). The abundances of all these classes were generally lower in RF, where *Betaproteobacteria* dominated (ca. 40%), followed by *Gammaproteobacteria* (ca. 10%). TF contained most of these classes, with similar abundances. The LEfSe algorithm identified indicator groups at different taxonomic levels associated with leaves, TF, and RF (Figure 4). At the class level, *Verrucomicrobia* and *Planctomycetes* were exclusively associated with TF, whereas *Actinobacteria* were associated with leaves. *Bacteroidetes* were present in both TF and leaves samples, though different taxa were associated to each sample type. Finally, *Proteobacteria* were ubiquitous across all samples, though specific taxa within *Betaproteobacteria* and *Gammaproteobacteria* were only associated to RF/TF water, while within *Alphaproteobacteria* we found specific taxa associated to all sample types (Figure 4). The abundances of OTUs were correlated most strongly between RF and TF samples ($R_s = 0.49$, $p < 0.001$). In contrast, OTUs abundant on leaves were not necessarily abundant in TF (Supporting Figure S5).

Taxa of nitrifying microbes were tentatively identified based on the 16S rRNA gene identity (> 98%) with known AOA and AOB species (Figure S6). The AOB species identified were related to *Nitrosomonas* and *Nitrosospira*, while AOA species were closely related to *Nitrososphaera*. Nitrifiers were detected mainly in some of the foliar samples and at both canopy positions (Figure S6). AOB species were also detected in a TF sample collected in December.

3.3. Changes in the *amoA* genes across samples and over time

We quantified the abundance of the *amoA* gene responsible for the first step of nitrification in both bacteria (AOB) and Archaea (AOA). The abundance of genes was expressed as the number of copies per nanogram (ng) of microbial DNA obtained from each sample (Behrens *et al.*, 2008) as described in the supplementary information. Archaeal *amoA* was more abundant than bacterial *amoA* across water samples (Figure 5, panels a and b). *amoA* in AOB was more difficult to detect in the foliar samples (only 2 of 8 samples), but *amoA* in AOA was as abundant on foliar surfaces as in RF and TF water (relative to the month, November, when the foliar samples were collected; Figure S7). The presence of this functional gene tended to be higher on the leaves collected from branches in the lower canopy positions, although the difference was not significant due to the high variability (Figure S8). The abundance of archaeal nitrifiers was in the same range

of values in RF and TF. However, AOA in TF tended to decrease by 16.06 % across months during the study period (R^2= 0.45, t= -2.71, p< 0.05, df= 9), while it increased by 17.46% for AOB (R^2=0.54, t=2.43, p=0.05, df=5). The limited number of observations (n=5) does not allow drawing statistically robust conclusions on temporal trend for functional genes in RF water, particularly for AOB, which were less abundant in our samples (e.g., repeated qPCR analyses allowed to detect AOB in RF only for 3 out of 5 dates, Figure 5).

3.4. Isotopic composition of nitrate in RF and TF and the mass-balance approach

Oxygen isotope ratios measured in NO_3^- generally did not differ significantly between RF and TF (the values of $\delta^{18}O$ and $\Delta^{17}O$ in RF often overlapped with those in TF), whereas NO_3^- had more positive $\delta^{15}N$ values in TF than RF (t= -3.47, p< 0.05). As for the seasonal trend, in the case of TF both $\delta^{18}O$ (slope= 15.77‰ month^{-1} ± 3.07, R^2= 0.77, p< 0.0001) and $\Delta^{17}O$ (slope= 3.48‰ month^{-1} ± 0.55, R^2= 0.83, p< 0.0001) increased over time, whereas $\delta^{15}N$ decreased (slope= -1.48‰ month^1 ± 0.33, R^2= 0.71, p< 0.001) (Figure 6 panels a-c). Similar to functional gene data, the limited number of observations (n=4), prevented exploring trends for stable isotopes in NO_3^- from RF water.

On average, the two-end mixing model based on $\Delta^{17}O$ (see Materials and Methods) indicated that the atmosphere was the dominant source of NO_3^- (mean f_{Atm}= 0.96 ± 0.09), with a low proportion from biological nitrification (f_{Bio}= 0.04 ± 0.09). The biological fraction tended to decrease over time, with the highest biological activity in the canopy in August (i.e. ≈ 0.2, or 20%) and partially in September (≈ 8%), while values decreased to near zero as winter approached, following a nonlinear trend (Figure 7).

4. Discussion

Our study provides a mechanistic understanding of the difference in NO_3^- fluxes between RF and TF, which does not include only the contribution of dry N_{dep} as source of NO_3 reaching the soil as TF. It also identifies tree canopies as an important habitat for microbial communities, including -- but not limited to -- species involved in nitrification.

4.1 Assessing N fluxes at La Castanya: types, magnitudes, and sources

Wet deposition as derived from N fluxes in RF was in the same range of values reported in previous studies at La Castanya (Aguillaume *et al.*, 2016; Avila *et al.*, 2017). The N fluxes in the

form of NO_3^- were larger in TF than RF during the study period, suggesting that dry deposition may have contributed substantially to total NO_3^- deposition. The site is in a remote area, but the higher N as NO_3^- fluxes in TF may have been due to the influence of NO_x emissions from the urban area of Barcelona (40 km from the site). N in the form of NH_4^+ is preferentially retained by tree canopies (Adriaenssens *et al.*, 2011), which may account for the small differences seen between RF and TF in NH_4-N.

The significant contribution of dry deposition to NO_3^- TF fluxes was also supported by the difference in $\delta^{15}N$-NO_3 between RF and TF. Indeed, the $\delta^{15}N$ values of NO_3 in dry deposition tend to be higher than in bulk precipitation (Heaton *et al.*, 1997; Beyn *et al.*, 2015). Washing of dry NO_3^- from the canopy is then reflected in more ^{15}N-enriched NO_3^- in TF than RF. Both N and O isotopic ratios had strong seasonal pattern, with NO_3^- in TF becoming more depleted in ^{15}N (i.e., more negative $\delta^{15}N$ values) and enriched in ^{18}O and ^{17}O (higher $\delta^{18}O$ and $\Delta^{17}O$ values) going from the summer towards the beginning of the winter. There are several reasons that could explain this pattern. Changes in $\delta^{15}N$ in NO_3^- could be attributed to seasonal shifts in NO_x sources (Kendall *et al.*, 2007 and references therein; Beyn *et al.*, 2015). Higher $\delta^{18}O$ and $\Delta^{17}O$ values in colder than warmer months have been observed previously (Michalski *et al.*, 2004; Savard *et al.*, 2018). It is likely that this increase does not indicate changes in NO_x sources but contributions from tropospheric water (for $\delta^{18}O$), ozone formation, and different oxidation pathways (e.g. with the N_2O_5 hydrolysis pathway predominant in winter) for $\Delta^{17}O$, all of which depend on temperature and solar radiation (Tsunogai *et al.*, 2010; Michalski *et al.*, 2012; Savard *et al.*, 2018).

4.2 Discriminating between atmosphere and leaf microbes as a source of nitrate in TF fluxes

The isotopic and flux data provided evidence of a large input of dry NO_3^- deposition at the site, but we were nonetheless able to detect biological activity as a source of NO_3^- in some of the investigated months. We found isotopic evidence of NO_3^- derived from nitrification in the canopies of the holm oak trees in August (about 20%), after a severe drought, and to a lower extent in September (about 8%), while it decreased and approached zero towards the beginning of the winter. This seasonal partitioning between biologically and atmospherically derived NO_3^- in TF inferred from $\Delta^{17}O$ data was also apparent in the temporal trend in the abundance of archaeal *amoA* gene. Curiously, a similar behaviour has been observed in a Mediterranean dry stream

where microbial ammonia oxidation activity in surface sediments and nitrate export to the fluvial networks is strongly shaped by seasonal flow cessation and drying (Merbt *et al.*, 2016). Both bacterial and archaeal nitrifiers were present in the phyllosphere, as confirmed by the two independent, yet complementary, approaches we used, i.e., qPCR and taxonomic assignment based on 16S rRNA gene analyses. However, AOA were more abundant than AOB, according to the quantification of the *amoA* gene through qPCR. Therefore, both f_{Bio} and the abundance of archaeal *amoA* in TF tended to decrease from the summer peak towards the beginning of winter, though the former followed a non-linear trend. These results suggest that archaea may be responsible for nitrification in the tree canopies at our site under the hot and dry summer conditions. The seasonal pattern we observed for both f_{Bio} and archaeal *amoA* suggest that the prolonged hot and dry conditions favoured the deposition and accumulation of dry atmospheric NH_x on the canopy surface, which, in turn, may have increased biological activity. Evidence from soil-based studies suggests that AOA prefers more oligotrophic conditions, even though both AOA and AOB respond positively to increases in N availability (Hatzenpichler, 2012; Carey *et al.*, 2016). Whether and how atmospheric N_{dep} contributes to shifts between bacterial and archaeal nitrification in tree canopies is unknown and other-omic techniques (i.e., metaproteomic and transcriptomic) may be more appropriate to assess this aspect. Bacterial and archaeal nitrifiers may also differ in their responses to temperature, with archaea operating at higher temperatures than bacteria (Taylor *et al.*, 2016). This difference could be exacerbated in the phyllosphere, where microbes experience rapid and extreme changes in environmental conditions, particularly solar radiation and temperature (Vorholt, 2012). Holm oak is known as a thermo-tolerant tree species, able to support temporary heat stress up to 50 °C without losing its photosynthetic capacity (Trabaud & Methy, 1994).

The fraction of NO_3^- from biological transformation in the tree canopies was at the lower range of values reported in a previous study for beech and Scots pine trees in the UK (Guerrieri *et al.*, 2015). In this latter case, however, trees had been exposed to a higher level of NH_x deposition, from intensive pig farming, than the trees at our site. Our results nevertheless indicate that biological nitrification did occur, even under a low level of N_{dep}. Assuming the absence of biological transformations in tree canopies (e.g., in the CBM) may thus not always be correct. Indeed, if we assume that 20% of the NO_3 in August is from nitrification, then the total NH_4 input, which includes dry deposition, should consequently be 20% higher than measured concentrations

and the CBM.

A number of studies have demonstrated the potential of $\Delta^{17}O$ as an unambiguous tracer of atmospheric NO_3^-, though most of them investigated atmospheric processes and/or sources of NO_3^- in soil solution (e.g., Michalski *et al.*, 2003; Costa *et al.*, 2011; Michalski *et al.*, 2012). Our study supports (as does Guerrieri *et al.*, 2015) the usefulness of this approach to explore processes during interactions between atmospheric N and tree canopies and to depict the microbial activity of nitrifiers in the phyllosphere (indicated by the genetic analyses). More studies, however, are needed to improve the use of $\Delta^{17}O$ for detecting and quantifying f_{Bio} across different tree species and along broader climate and N deposition gradients. One limitation in our approach is that any signal of microbial activity during dry days can be diluted by the actual discharge of atmospheric N deposition during a precipitation event. The method by which TF water is processed, e.g., by pooling water from multiple precipitation events within a month, may add further uncertainty. This could partially explain why occasional values <0 or >1 were obtained for $f NO_3^-$ from biological activity and atmosphere, respectively. Intensifying sampling (e.g., using ion-exchange resins directly in the field, see e.g., Fenn & Poth, 2004; Decina *et al.*, 2018) and/or combining seasonal estimates of $\Delta^{17}O$ on wet and dry deposition could help elucidate the dynamics of microbial activity in the phyllosphere, better quantify f_{Bio} and determine the effect of environmental conditions.

4.3 Microbial life hidden in tree canopies: structure, composition, origin and fate

Our study is the first to provide indications on microbial communities in the phyllosphere of one of the most important species in Mediterranean forests. Moreover, it adds to the few studies using NGS (next-generation sequencing) and metabarcoding analyses, demonstrating that leaves sampled from tree canopies can harbour a highly diverse microbial community on their surface. General taxa identified on the foliar surfaces of holm oak at La Castanya were similar to those reported for deciduous species in a temperate forest in Quebec (Laforest-Lapointe *et al.*, 2016) and for >50 species in a tropical forest in Panama (Kembel et al. 2014). *Alpha-* and *Betaproteobacteria*, *Sphingobacteriia*, and *Actinobacateria* are amongst the overlapping dominant taxa. While *Gammaproteobacteria* are abundant only on the leaves of tropical species (Kembel et al., 2014), *Cytophagia* are abundant predominantly in the phyllosphere of Mediterranean species and temperate deciduous species in Quebec (Laforest-Lapointe *et al.*, 2016), suggesting a

difference in host plant/microbiome composition based on vegetation type and forest biome. More studies, however, are needed to better characterize the leaf microbiome of holm oak across the Mediterranean region and, more in general, to investigate the foliar microbial composition of different species across different forest types. Such studies are now relatively easy and fast to carry out due to the advent of NGS techniques and high-computation facilities.

Diversity was high (both OTU richness and the Shannon index) across our samples, with microbial communities more diverse in TF and the phyllosphere than RF. This suggests that TF communities represent a mixture of bacteria from rain and enriched by those in the canopies, which are washed from the canopies during rain. Interestingly, RF and leaf samples shared some of the taxa identified, which were then not found in TF water, suggesting that tree canopies may act as filter not only for atmospheric chemical compounds, but also for microbes carried by precipitation. Nevertheless, our results indicate that the ecological importance of TF fluxes goes beyond the input of water and chemicals passing through canopies to the soil (Rosier *et al.*, 2015). Indeed microbial cells washed from the canopies via TF join (or alter) the microbial communities in the soil (Van Stan & Stubbins, 2018), and represent also an important input of nutrients to the soil, such as carbon (C), N, and phosphorus. Bittar *et al.*, (2018) estimated a flux of 1.5×10^{16} cells ha^{-1} year^{1} to the soil from TF in a subtropical oak-cedar forest in South-eastern USA, which corresponded to a contribution of organic C from the phyllosphere to the soil of 0.6-2.3 kg ha^{-1} year^{-1}.

The high variance (i.e., beta-diversity) in both the structure and composition of the microbial communities in RF has been consistently associated with the origin of deposition coupled to the seasonal circulation of atmospheric air masses (Cáliz *et al.*, 2018), and not to the type of deposition (i.e. dry or wet) (Triadó-Margarit *et al.*, 2019). On the other hand, Reche *et al.,* (2018) observed that the rates of bacterial deposition at two locations at the peak of Sierra Nevada in South-eastern Spain were higher during rain with the intrusion of dust from the Sahara Desert (i.e. air masses from northern Africa) than during only dry deposition event. The intrusion of Saharan dust may enrich the air mass with nutrients and allochthonous microbiome components (Cáliz *et al.*, 2018) and change the composition of bacterial communities, with important implications for aquatic (Hervàs *et al.*, 2009; Peter *et al.*, 2014; Itani & Smith, 2016) and terrestrial (Yu *et al.*, 2015) ecosystems. Origins of air masses reaching our site were quite different across the investigated months (Figure S9), which may help explaining the high variability in the structure and composition of microbial communities in RF over time. Indeed, contribution of air masses

coming from the South, carrying dust from the Sahara, was quite obvious for November and December months, whereas air masses with different origins contributed to precipitation events in September and October. As for August, although air trajectory analysis suggests that precipitation events for this month had Northern origin, an important dust mass moved from North Africa up to the Atlantic just a few days before the rain event occurred (Figure S10). This may explain why we observed microbial communities in August RF to be closer to those sampled in November and December RF rather than those collected in September and October.

Conclusion

Our study sheds light on the magnitude and temporal changes of nitrification in tree canopies, probably a widespread process, given the global distribution of phyllospheric microbes (an estimated terrestrial surface leaf area of 6.4×10^8 km^2, Morris & Kinkel 2002), and exacerbated by the large amounts of reactive N in the atmosphere caused by human activities. We showed that canopy retention of NH_4^+ and leaching of dry NO_3^- deposited onto tree canopies accounted for the observed dynamics of NO_3^- and NH_4^+ fluxes between RF and TF. By using $\Delta^{17}O$, however, we were able to detect biological activity in the canopy, particularly in August (and September with a lower magnitude) after a long drought, and results from qPCR suggested archaeal nitrifiers as responsible for it. Finally, we found that holm oak tree canopies host a highly diverse community of microbes, which partially affected the structure and composition of the microbes in TF and consequently in the soil. Microbiologists have overlooked for a long time the study of ammonia-oxidizers in the phyllosphere (Fernandez-Guerra & Casamayor, 2012). Results from this study indicate that biological nitrification does not occur only in the rhizosphere, highlighting the potential global role that the phyllosphere can play in nitrification and, more in general, in nutrient cycling (Nadkarni, Parker, Lowman, 2011). A more in-depth analysis of these processes will require a larger number of replicates, while further research will be needed to i) confirm the observed seasonal changes at larger spatial and temporal scale and ii) better quantify the relative contributions of canopy bio-transformations to forest N cycling.

Acknowledgments

Author contribution

RG, AA, MM and JP designed the study. LL, RG and AA were responsible for sample collection and preparation for genetic, chemical and isotope analyses. AB conducted DNA sequencing with Illumina, SM carried out the qPCR analyses, and GM carried out the isotope analyses. AA elaborated N flux data and air trajectory data, JC processed the raw DNA sequences as obtained from the Illumina and carried out bioinformatic and statistical analyses with the support of EOC, while RG was responsible of processing isotope and functional gene data. RG wrote the manuscript with contributions from all the co-authors.

Data Availability

The genetic dataset from 16S sequence analyses is available at the National Center for Biotechnology Information Sequence Read Archive under accession no. PRJNA560873. Isotope and functional gene data are available from the Dryad Digital Repository: https://doi.org/10.5061/dryad.3cq6127

References

Adriaenssens S, Staelens J, Wuyts K, de Schrijver A, Van Wittenberghe S, Wuytack T, Kardel F, Verheyen K, Samson R, Boeckx P. 2012. Foliar nitrogen uptake from wet deposition and the relation with leaf wettability and water storage capacity. *Water Air Soil*

*Pollut*ion, 219, 43–57.

Adriaenssens S, Staelens J, Baeten L, Verstraeten A, Boeckx P, Samson R, Verheyen K. 2013. Influence of canopy budget model approaches on atmospheric deposition estimates to forests. *Biogeochemistry* 116 (1-3): 215-229.

Aguillaume L, Izquieta-Rojano S, García-Gómez H, Elustondo D, Santamaría J, Alonso R, Avila A. 2017. Dry deposition and canopy uptake in Mediterranean holm-oak forests estimated with a canopy budget model: A focus on N estimations. *Atmospheric Environment*, 152, 191–200.

Aguillaume L, Rodrigo A, Avila A. 2016. Long-term effects of changing atmospheric pollution on throughfall, bulk deposition and streamwaters in a Mediterranean forest. *Science of The Total Environment*, 544, 919–928.

Anderson MJ. (2001). A new method for non-parametric multivariate analysis of variance. *Austral Ecology*, 26 (1), 32-46.

Andrews JH, Harris RF. 2000. The ecology and biogeography of microorganisms on plant surfaces. *Annu. Rev. Phytopathol.*, 38,145-80.

Avila A. 1996. Time trends in the precipitation chemistry at a montane site in north-eastern Spain for the period 1983-1994. Atmos. Environ., 30, 1363–1373.

Avila A, Aguillaume L, Izquieta-Rojano S, García-Gómez H, Elustondo D, Santamaría JM, Alonso R. 2017. Quantitative study on nitrogen deposition and canopy retention in Mediterranean evergreen forests. *Environmental Science and Pollution Research*, 24, 26213–26226.

Behrens S, Azizian MF, McMurdie PJ, Sabalowsky A, Dolan ME, Semprini L, Spormann AM. 2008. Monitoring abundance and expression of "Dehalococcoides" species chloroethene-reductive dehalogenases in a tetrachloroethene-dechlorinating flow column. *Applied and Environmental Microbiology* 74, 5695–5703.

Beyn F, Volker M, Armin A, Dähnke K. 2015. Do N-isotopes in atmospheric nitrate deposition reflect air pollution levels?,Atmospheric Environment, 107, 281-288.

Bittar TB, Pound P, Whitetree A, Moore LD, Stan JTV. 2018. Estimation of Throughfall and Stemflow Bacterial Flux in a Subtropical Oak-Cedar Forest. *Geophysical Research Letters*, 45, 1410–1418.

Cáliz J, Triadó-Margarit X, Camarero L, Casamayor EO. 2018. A long-term survey unveils strong seasonal patterns in the airborne microbiome coupled to general and regional

atmospheric circulations. *Proc Natl Acad Sci U.S.A.* 115 (48), 12229-12234.

Carey CJ, Dove NC, Beman JM, Hart SC, Aronson EL. 2016. Meta-analysis reveals ammonia-oxidizing bacteria respond more strongly to nitrogen addition than ammonia-oxidizing archaea. *Soil Biology and Biochemistry*, 99, 158–166.

Casciotti KL, Sigman DM, Hastings MG, Böhlke JK, Hilkert A. 2002. Measurement of the Oxygen Isotopic Composition of Nitrate in Seawater and Freshwater Using the Denitrifier Method. *Analytical Chemistry*, 74, 4905–4912.

Costa AW, Michalski G, Schauer AJ, Alexander B, Steig EJ, Shepson PB. 2011. Analysis of atmospheric inputs of nitrate to a temperate forest ecosystem from $\Delta^{17}O$ isotope ratio measurements. *Geophysical Research Letters*, 38.

Dail DB, Hollinger DY, Davidson EA, Fernandez I, Sievering HC, Scott NA, Gaige E. 2009. Distribution of nitrogen-15 tracers applied to the canopy of a mature spruce-hemlock stand, Howland, Maine, USA. *Oecologia,* 160, 589-599.

Decina SM, Templer PH, & Hutyra LR. 2018. Atmospheric Inputs of Nitrogen, Carbon, and Phosphorus across an Urban Area: Unaccounted Fluxes and Canopy Influences, *Earth's Future*, 6, 134–148

Delmotte N, Knief C, Chaffron S, Innerebner G, Roschitzki B, Schlapbach R, von Mering C, Vorholt JA. 2009. Community proteogenomics reveals insights into the physiology of phyllosphere bacteria. *Proceedings of the National Academy of Sciences*, 106, 16428–16433.

Dise NB, Ashmore M, Belyazid S, Bleeker A, Bobbink R, de Vries W, Erisman JW, Spranger T, Stevens CJ, van den Berg L. 2011. Nitrogen as a threat to European terrestrial biodiversity. In: Sutton MA, Howard CM, Erisman JW, Billen G, Bleeker A, Grennfelt P, van Grinsven H, Grizzetti B, eds. *The European nitrogen assessment sources, effects, and policy perspectives* Cambridge University Press, pp 463-494.

Dixon P. 2003. VEGAN, a package of R functions for community ecology. *Journal of Vegetation Science*, 14, 927.

Draaijers G, Erisman J, Spranger T, Wyers G. 1996. The application of throughfall measurements for atmospheric deposition monitoring. *Atmospheric Environment*, 30, 3349–3361.

Edgar RC. 2013. UPARSE: highly accurate OTU sequences from microbial amplicon reads. *Nature Methods*, 10, 996–998.

Edgar RC, Flyvbjerg H. 2015. Error filtering, pair assembly and error correction for next-generation sequencing reads. *Bioinformatics*, 31, 3476–3482.

Erisman JW, Grinsven HV, Grizzetti B, Bouraoui F, Powlson D, Sutton MA, Bleeker A, Reis S. 2011. The European nitrogen problem in a global perspective. In: Sutton MA, Howard CM, Erisman JW, Billen G, Bleeker A, Grennfelt P, van Grinsven H, Grizzetti B, eds. *The European nitrogen assessment sources, effects, and policy perspectives* Cambridge University Press, 9–31.

Fenn ME, Poth MA. 2004. Monitoring Nitrogen Deposition in Throughfall Using Ion Exchange Resin Columns. *Journal of Environment Quality*, 33, 2007.

Fenn ME, Ross CS, Schilling SL, Baccus WD, Larrabee MA, Lofgren RA. 2013. Atmospheric deposition of nitrogen and sulfur and preferential canopy consumption of nitrate in forests of the Pacific Northwest, USA. *Forest Ecology and Management*, 302, 240–253.

Fernandez-Guerra A, Casamayor EO. 2012. Habitat-Associated Phylogenetic Community Patterns of Microbial Ammonia Oxidizers" PlosONE doi.org/10.1371/journal.pone.0047330

Ferretti M, Marchetto A, Arisci S, Bussotti F, Calderesi M et al. 2014. On the tracks of Nitrogen deposition effects on temperate forests at their southern European range - an observational study from Italy. *Global Change Biology*, 20, 3423–3438.

Galloway JN, Cowling EB. 2003. Reactive Nitrogen and The World: 200 Years of Change *Ambio*, 31 (2), 64-71.

García-Gómez H, Aguillaume L, Izquieta-Rojano S, Valiño F, Avila A, Elustondo D, Santamaría JM, Alastuey A, Calvete-Sogo H, González-Fernández I, Alonso R. 2016. Atmospheric pollutants in peri-urban forests of Quercus ilex : evidence of pollution abatement and threats for vegetation. *Environ Sci Pollut Res*, 23, 6400-6413.

Griffith KT, Ponette-González AG, Curran LM, Weathers KC. 2015. Assessing the influence of topography and canopy structure on Douglas fir throughfall with LiDAR and empirical data in the Santa Cruz mountains, USA. Environ Monit Assess 187: 270.

Guerrieri R, Vanguelova EI, Michalski G, Heaton THE, Mencuccini M. 2015. Isotopic evidence for the occurrence of biological nitrification and nitrogen deposition processing in forest canopies. *Global Change Biology*, 21, 4613–4626.

Hatzenpichler R. 2012. Diversity, Physiology, and Niche Differentiation of Ammonia-Oxidizing Archaea. *Applied and Environmental Microbiology*, 78, 7501–7510.

Heaton THE, Spiro B, Madeline S, Robertson C. 1997. Potential canopy influences on the

isotopic composition of nitrogen and sulphur in atmospheric deposition. *Oecologia*, 109, 600-607.

Hervàs A, Camarero L, Reche I, Casamayor EO. 2009. Viability and potential for immigration of airborne bacteria from Africa that reach high mountain lakes in Europe. *Environmental Microbiology*, 11, 1612–1623.

Högberg P. 1997. Tansley Review No. 95. ^{15}N natural abundance in soil-plant systems. *New Phytologist*, 137, 179–203.

Houle D, Marty C, Duchesne L. 2015. Response of canopy nitrogen uptake to a rapid decrease in bulk nitrate deposition in two eastern Canadian boreal forests. *Oecologia,* 177, 29–37

Itani GN, Smith CA. 2016. Dust Rains Deliver Diverse Assemblages of Microorganisms to the Eastern Mediterranean. *Scientific Reports*, 6, 22657

Kaiser J, Hastings MG, Houlton BZ, Röckmann T, Sigman DM. 2007. Triple Oxygen Isotope Analysis of Nitrate Using the Denitrifier Method and Thermal Decomposition of N2O. *Analytical Chemistry*, 79, 599–607.

Kembel SW, O'connor TK, Arnold HK, Hubbell SP, Wright SJ, Green JL. 2014. Relationships between phyllosphere bacterial communities and plant functional traits in a neotropical forest. *Proceedings of the National Academy of Sciences*, 111, 13715–13720.

Kendall C, Elliott EM, Wankel SD. 2007. Tracing anthropogenic inputs of nitrogen to ecosystems. In: Michener R, Lajtha K eds *Stable Isotopes in Ecology and Environmental Science*. Blackwell Publishing, Boston, 375–449.

Laforest-Lapointe I, Messier C, Kembel SW. 2016. Tree phyllosphere bacterial communities: exploring the magnitude of intra- and inter-individual variation among host species. *PeerJ*, 4:e2367 https://doi.org/10.7717/peerj.2367.

Lambais MR, Crowley DE, Cury C, Büll RC, Rodrigues RR. 2006. Bacterial Diversity in Tree Canopies of the Atlantic Forest. *Science*, 312, 1917.

Legendre P, Gallagher ED. 2001. Ecologically meaningful transformations for ordination of species data. *Oecologia*, 129, 271–280.

Lindberg SE, Lovett GM, Richter DD, Johnson DW. 1986. Atmospheric deposition and canopy interactions of major ions in a forest. *Science*, 231, 141-145

Lindow SE, Brandl MT. 2003. Microbiology of the Phyllosphere. *Applied and Environmental Microbiology*, 69, 1875–1883.

Magnani F, Mencuccini M, Borghetti M, Berbigier P, Berninger F, Delzon S, Grelle A, Hari

P, Jarvis PG, Kolari P, et al. 2007. The human footprint in the carbon cycle of temperate and boreal forests. *Nature*, 447, 849–851.

Matsuhisa Y, Goldsmith JR, Clayton RN. 1978. Mechanisms of hydrothermal crystallization of quartz at 250°C and 15 kbar. *Geochimica et Cosmochimica Acta*, 42, 173–182.

Merbt SN, Proia L, Prosser JI, Martí E, Casamayor EO, von Schiller D. 2016. Stream drying drives microbial ammonia oxidation and first-flush nitrate export. *Ecology,* 97, 2192-2198

Michalski G, Savarino J, Böhlke JK, Thiemens M. 2002. Determination of the Total Oxygen Isotopic Composition of Nitrate and the Calibration of a $\Delta^{17}O$ Nitrate Reference Material. *Analytical Chemistry*, 74, 4989–4993.

Michalski G, Scott Z, Kabiling M, Thiemens MH. 2003. First measurements and modeling of $\Delta^{17}O$ in atmospheric nitrate. *Geophysical Research Letters*, 30, 1870, doi:10.1029/2003GL017015.

Michalski G, Böhlke J, Thiemens M. 2004. Long term atmospheric deposition as the source of nitrate and other salts in the Atacama Desert, Chile: New evidence from mass-independent oxygen isotopic compositions. *Geochimica et Cosmochimica Acta*, 68, 4023–4038.

Michalski G, Bhattacharya SK, Mase DF. 2012. Oxygen isotope dynamics of atmospheric nitrate and its precursor molecules. *Handbook of Environmental Isotope Geochemistry*, Springer, pp. 613-635.

Miller MF. 2002. Isotopic fractionation and the quantification of 17 O anomalies in the oxygen three-isotope system. *Geochimica et Cosmochimica Acta*, 66, 1881–1889.

Morris CE, Kinkel LL. 2002. Fifty years of phyllosphere microbiology: significant contributions to research in related fields. In Phyllosphere Microbiology ed. Lindow, S.E., Hecht-Poinar, E.I. and Elliott, V.J. pp. 365–375 St Paul, USA: APS Press.

Moyes AB, Kueppers LM, Pett-Ridge J, Carper DL, Vandehey N, O'neil J, Frank AC. 2016. Evidence for foliar endophytic nitrogen fixation in a widely distributed subalpine conifer. *New Phytologist*, 210, 657–668.

Mustajärvi K, Merilä P, Derome J, Lindroos A-J, Helmisaari H-S, Nöjd P, Ukonmaaho L. 2008. Fluxes of dissolved organic and inorganic nitrogen in relation to stand characteristics and latitude in Scots pine and Norway spruce stands in Finland. *Boreal Environment Research*, 13 (Suppl. B), 3–21.

Nadelhoffer KJ, Emmett BA, Gundersen P et al. 1999. Nitrogen deposition makes a minor contribution to carbon sequestration in temperate forests. *Nature*, 398, 145–148.

Nadkarni N, Parker G, Lowman M. 2011. Forest canopy studies as an emerging eld of science. *Annals of Forest Science*, 68 (2), 217-224

Papen H, Geβler A, Zumbusch E, Rennenberg H. 2002. Chemolithoautotrophic Nitrifiers in the Phyllosphere of a Spruce Ecosystem Receiving High Atmospheric Nitrogen Input. *Current Microbiology*, 44, 56–60.

Pérez N, Pey J, Castillo S, Viana M, Alastuey A, Querol X. 2008. Interpretation of the variability of levels of regional background aerosols in the Western Mediterranean. *Science of The Total Environment*, 407, 527–540.

Peter H, Hörtnagl P, Reche I, Sommaruga R. 2014. Bacterial diversity and composition during rain events with and without Saharan dust influence reaching a high mountain lake in the Alps. *Environ Microbiol Rep*, 6(6),618–24.

Ponette-González AG, Weathers KC, Curran LM. 2010. Tropical land-cover change alters biogeochemical inputs to ecosystems in a Mexican montane landscape. *Ecological Applications*, 20 (7), 1820-1837.

Quast C, Pruesse E, Yilmaz P, Gerken J, Schweer T, Yarza P, Peplies J, Glöckner FO. 2013. The SILVA ribosomal RNA gene database project: improved data processing and web-based tools. *Nucleic Acids Research*, 41 (D1): D590-D596.

R Core Team R: A language and environment for statistical computing 2016. R Foundation for Statistical Computing: Vienna, Austria.

Reche I, D'Orta G, Mladenov N, Winget DM, Suttle CA. 2018. Deposition rates of viruses and bacteria above the atmospheric boundary layer. *The ISME Journal*, 12, 1154–1162.

Reay DS, Dentener F, Smith P, Grace J, Feely R. 2008. Global nitrogen deposition and carbon sinks. *Nature Geoscience*, 1, 430–437.

Rico L, Ogaya R, Terradas J, Peñuelas J. 2014. Community structures of N^2-fixing bacteria associated with the phyllosphere of a Holm oak forest and their response to drought. *Plant Biology*, 16, 586–593.

Rosier CL, Moore LD, Wu T, Van Stan JT. 2015. Forest Canopy Precipitation Partitioning: An Important Plant Trait Influencing the Spatial Structure of the Symbiotic Soil Microbial Community. *Advances in Botanical Research*, 9 (75), 215-240.

Sah SP, Brumme R. 2003. Natural ^{15}N abundance in two nitrogen saturated forest ecosystems at Solling, Germany. *Journal of Forest Science*, 49, 512-522

Savard MM, Cole A, Vet R, Smirnoff A. 2018. The $\Delta^{17}O$ and $\delta^{18}O$ values of simultaneously

collected atmospheric nitrates from anthropogenic sources- Implications for polluted air masses. *Atmospheric Chemistry and Physics Discussions*, 18, 10373-10389

Schwarz MT, Oelmann Y, Wilcke W. 2011. Stable N isotope composition of nitrate reflects N transformations during the passage of water through a montane rain forest in Ecuador. *Biogeochemistry*, 102, 195–208.

Segata N, Izard J, Waldron L, Gevers D, Miropolsky L, Garrett WS, Huttenhower C. (2011). Metagenomic biomarker discovery and explanation. *Genome Biology*, 12 (6), R60.

Shokralla S, Spall JL, Gibson JF, Hajibabaei M. 2012. Next-generation sequencing technologies for environmental DNA research. *Molecular Ecology*, 21, 1794–1805.

Sparks JP. 2009. Ecological ramifications of the direct foliar uptake of nitrogen. *Oecologia*, 159, 1–13.

Triadó-Margarit X, Calíz J, Reche I, Casamayor E O. 2019. High similarity in bacterial bioaerosol compositions between the free troposphere and atmospheric depositions collected at high-elevation mountains. *Atmospheric Environment,* 203, 79-86.

Taylor AE, Giguere AT, Zoebelein CM, Myrold DD, Bottomley PJ. 2016. Modeling of soil nitrification responses to temperature reveals thermodynamic differences between ammonia-oxidizing activity of archaea and bacteria. *The ISME Journal*, 11, 896–908.

Templer PH, Weathers KC, Lindsey A, Lenoir K, Lindsay S. 2015. Atmospheric inputs and nitrogen saturation status in and adjacent to Class I wilderness areas of the northeastern US. *Oecologia,* 177, 5.

Trabaud L & Methy M (1994). Tolérance aux stress thermiques des feuilles et aire de répartition de Quercus ilex. *Ecologia Mediterranea*, XX, 77–85.

Tsunogai U, Komatsu DD, Daita S, Kazemi GA, Nakagawa F, Noguchi I, Zhang J. 2010. Tracing the fate of atmospheric nitrate deposited onto a forest ecosystem in Eastern Asia using $\Delta^{17}O$. *Atmos. Chem. Phys.*, 10, 1809-1820.

Vacher C, Hampe A, Porté AJ, Sauer U, Compant S, Morris CE. 2016. The Phyllosphere: Microbial Jungle at the Plant–Climate Interface. *Annual Review of Ecology, Evolution, and Systematics*, 47, 1–24.

Vanguelova E, Benham S, Pitman R, Moffat AJ, Broadmeadow M et al. 2010. Chemical fluxes in time through forest ecosystems in the UK − Soil response to pollution recovery. *Environmental Pollution*, 158, 1857–1869.

Van Stan JTV, Stubbins A. 2018. Tree-DOM: Dissolved organic matter in throughfall and

stemflow. *Limnology and Oceanography Letters*, 3, 199–214.

Vorholt JA. 2012. Microbial life in the phyllosphere. *Nature Reviews Microbiology*, 10, 828–840.

Wang Q, Garrity GM, Tiedje JM, Cole JR. 2007. Naïve Bayesian Classifier for Rapid Assignment of rRNA Sequences into the New Bacterial Taxonomy. *Appl Environ Microbiol*. DOI: 10.1128/AEM.00062-07.

Watanabe K, Kohzu A, Suda W, Yamamura S, Takamatsu T, Takenaka A, Koshikawa MK, Hayashi S, Watanabe M. 2016. Microbial nitrification in throughfall of a Japanese cedar associated with archaea from the tree canopy. *SpringerPlus*, 5. 1596.

Wickham H. 2016. ggplot2: Elegant Graphics for Data Analysis. Springer-Verlag New York.

Woods CL, Hunt SL, Morris DM, Gordon AM. 2012. Epiphytes influence the trans- formation of nitrogen in coniferous forest canopies. *Boreal Environment Research*, 17, 411–424.

Young ED, Galy A, Nagahara H. 2002. Kinetic and equilibrium mass-dependent isotope fractionation laws in nature and their geochemical and cosmochemical significance. *Geochimica et Cosmochimica Acta*, 66 (6), 1095-1104.

Yu H, Chin M, Yuan T, Bian H, Remer LA, Prospero JM, et al. 2015. The fertilizing role of African dust in the Amazon rainforest: A first multiyear assessment based on data from Cloud‐Aerosol Lidar and Infrared Pathfinder Satellite Observations. *Geophysical Research Letters*, 42, 1984–1991.

Figure captions

Figure 1. Nitrogen deposition over the investigated months. Temporal changes in NO_3—N and NH_4—N fluxes obtained from NO_3—N and NH_4—N concentrations in rainfall (RF) and throughfall (TF) from mid-summer to the beginning of winter in the holm oak forest at La Castanya, Spain.

Figure 2. Structure of bacterial communities across the different sample types. Non-metric multidimensional scaling (NMDS) ordination based on Bray-Curtis dissimilarities for the water and foliar samples (panel a, dot size corresponds to the Shannon index), and boxplots showing the distance to the centroids for each group of samples (panel b). Leaf_H and Leaf_L indicate foliar samples collected at top and intermediate/low canopy positions, respectively.

Figure 3. Bacterial composition across the different sample types. Relative abundances of bacterial classes of the phyllosphere (top and intermediate/bottom positions of the canopy), TF and RF in the holm oak forest at La Castanya. 'Others' includes all the classes with relative abundances < 0.5%. Leaf_H and Leaf_L indicate foliar samples collected at top and intermediate/low canopy positions, respectively.

Figure 4. Results from the Linear Discriminant Analysis Effect Size algorithm showing indicator microbial taxa for each sample type and five taxonomic levels from phylum (short circle in centre) to genus (large outer circle). White dots showed non-indicator taxa. Note the inverted colours for RF and foliar samples.

Figure 5. Changes in the abundance of the *amoA* functional gene involved in nitrification. Temporal changes in the abundances of the *amoA* genes in in ammonia-oxidizing bacteria (AOB) (panel a) and ammonia-oxidizing Archaea (AOA) (panel b). Abundance is expressed as the number of copies of the gene per nanogram (ng) of microbial DNA sample collected on the filters used to process RF and TF water.

Figure 6. Changes in stable nitrogen and oxygen isotope ratios in NO_3^-. Temporal changes in $\delta^{15}N$, $\delta^{18}O$, and $\Delta^{17}O$ in NO_3^- obtained from RF (n=4) and TF (n=10) from mid-summer to the beginning of winter in the holm oak forest at La Castanya. Note that isotope values in RF were similar to those obtained for TF in October and December ($\delta^{18}O$) and September, October and December ($\Delta^{17}O$), making difficult to distinguish them. Isotope values for November months are not available.

Figure 7. Atmospherically and biologically derived NO_3^-. Temporal changes in the fraction of NO_3^- (fNO_3^-) derived from microbial activity (Bio) and from atmospheric deposition (Atm) obtained by the mass-balance approach using $\Delta^{17}O$ in NO_3^- collected in TF and RF (ref. equation 3 in the Materials and Methods).
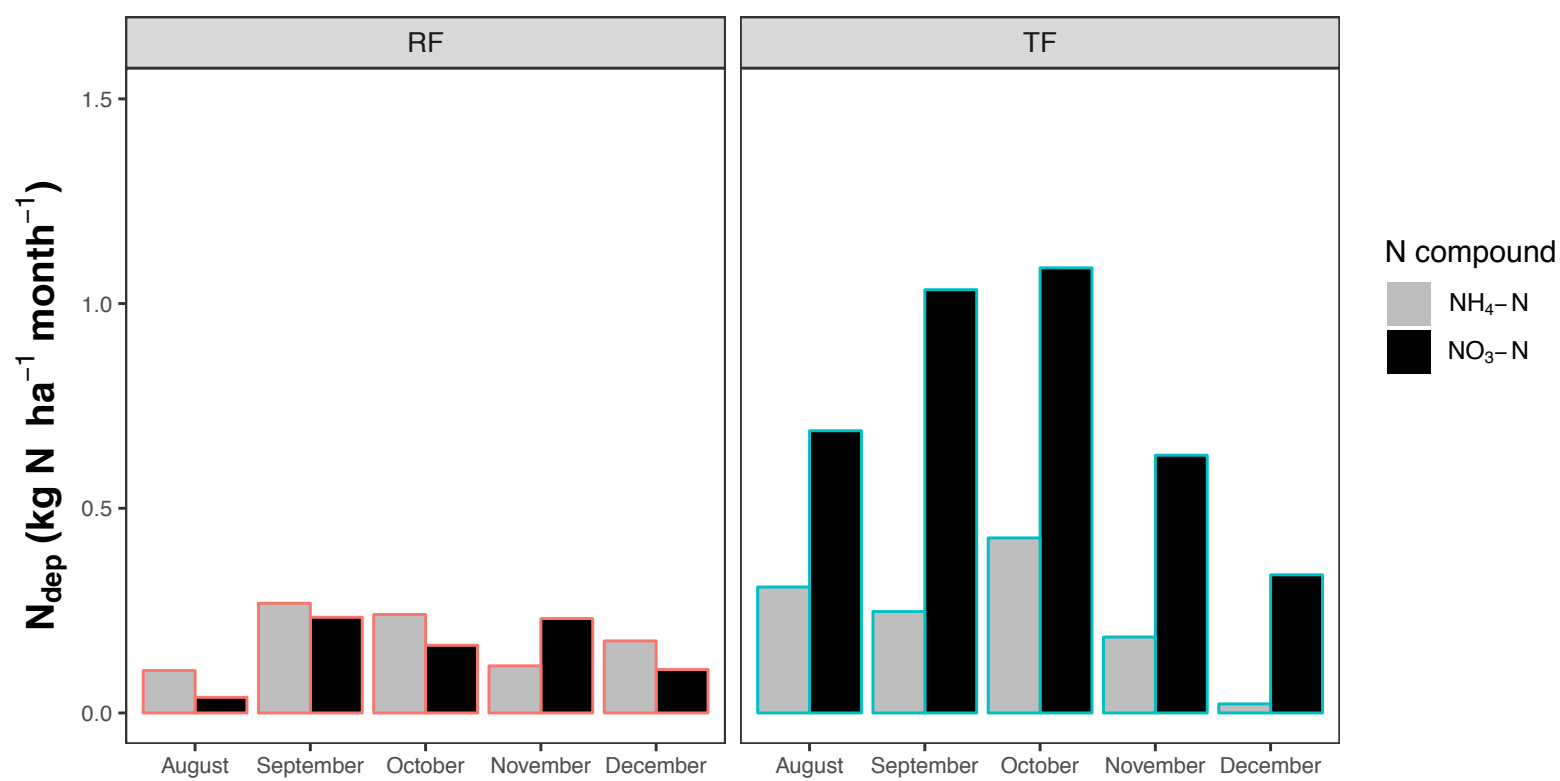
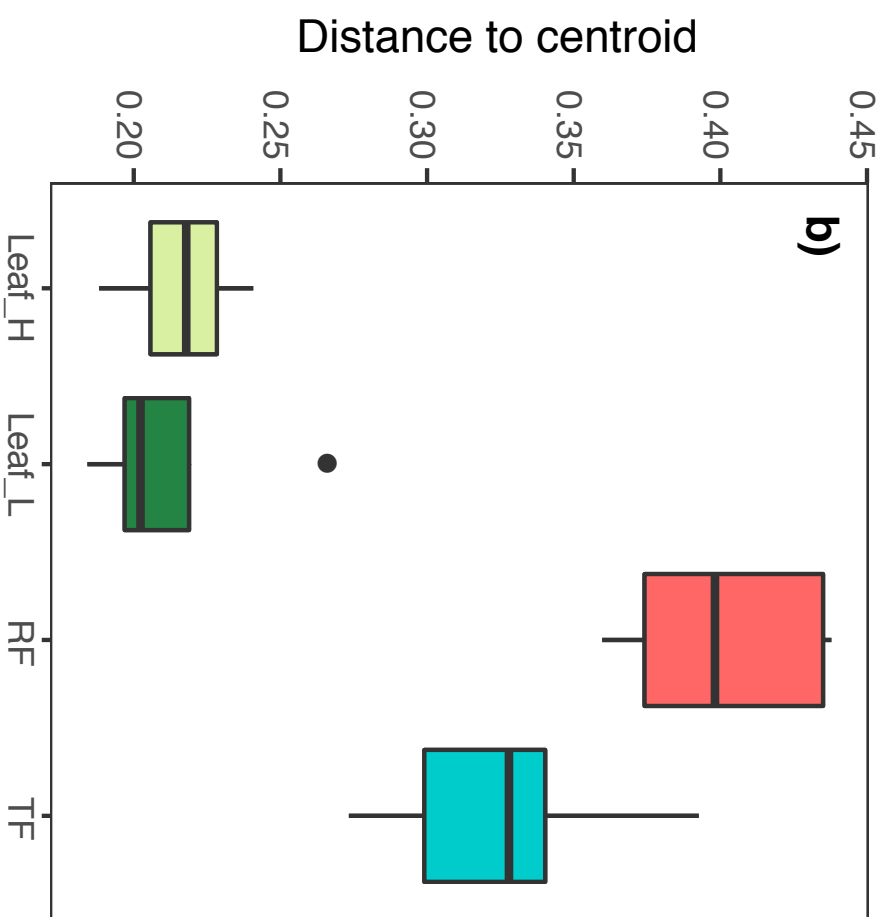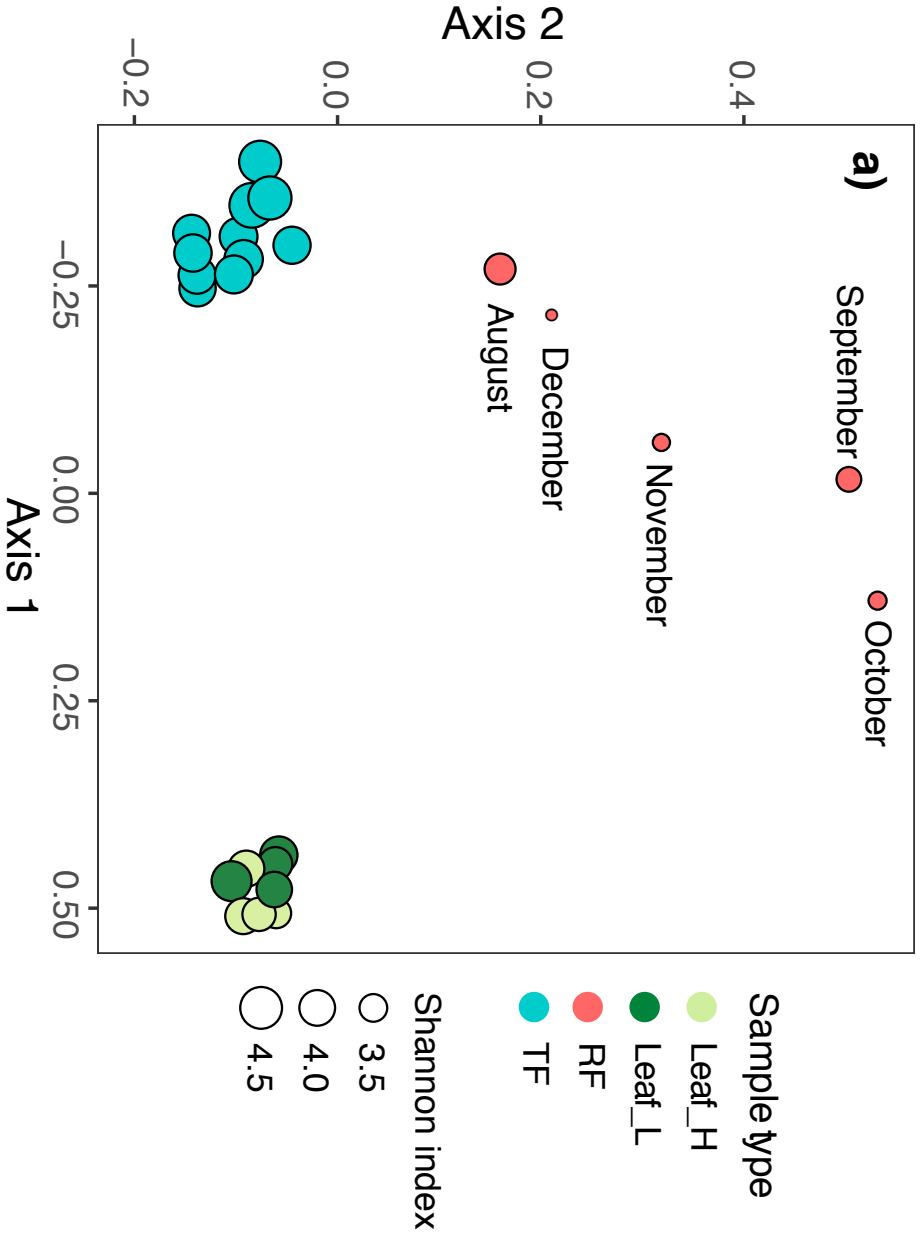**Table 1.** Site characteristics of La Castanya (Montseny mountain, Barcelona, NE Spain).

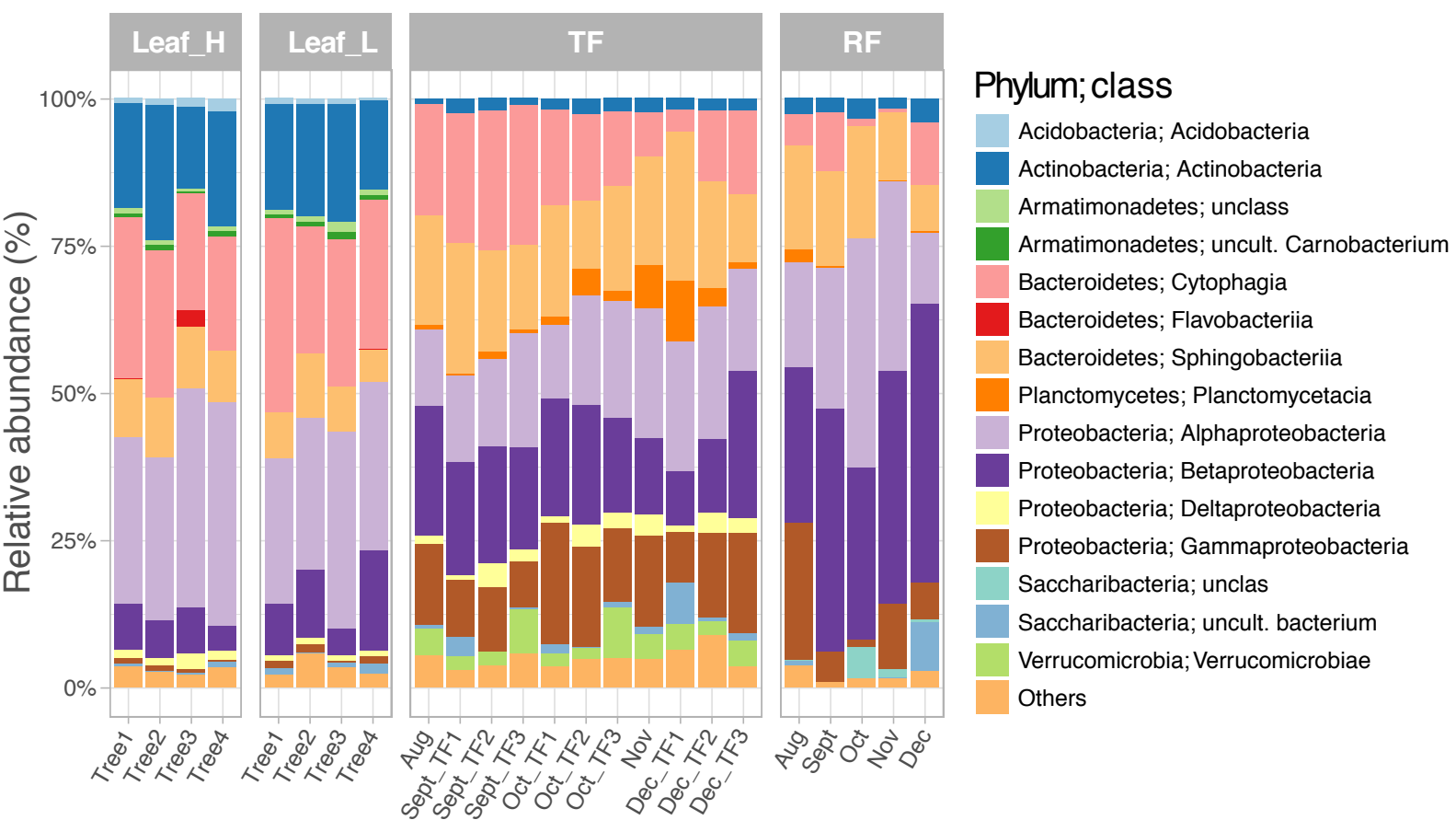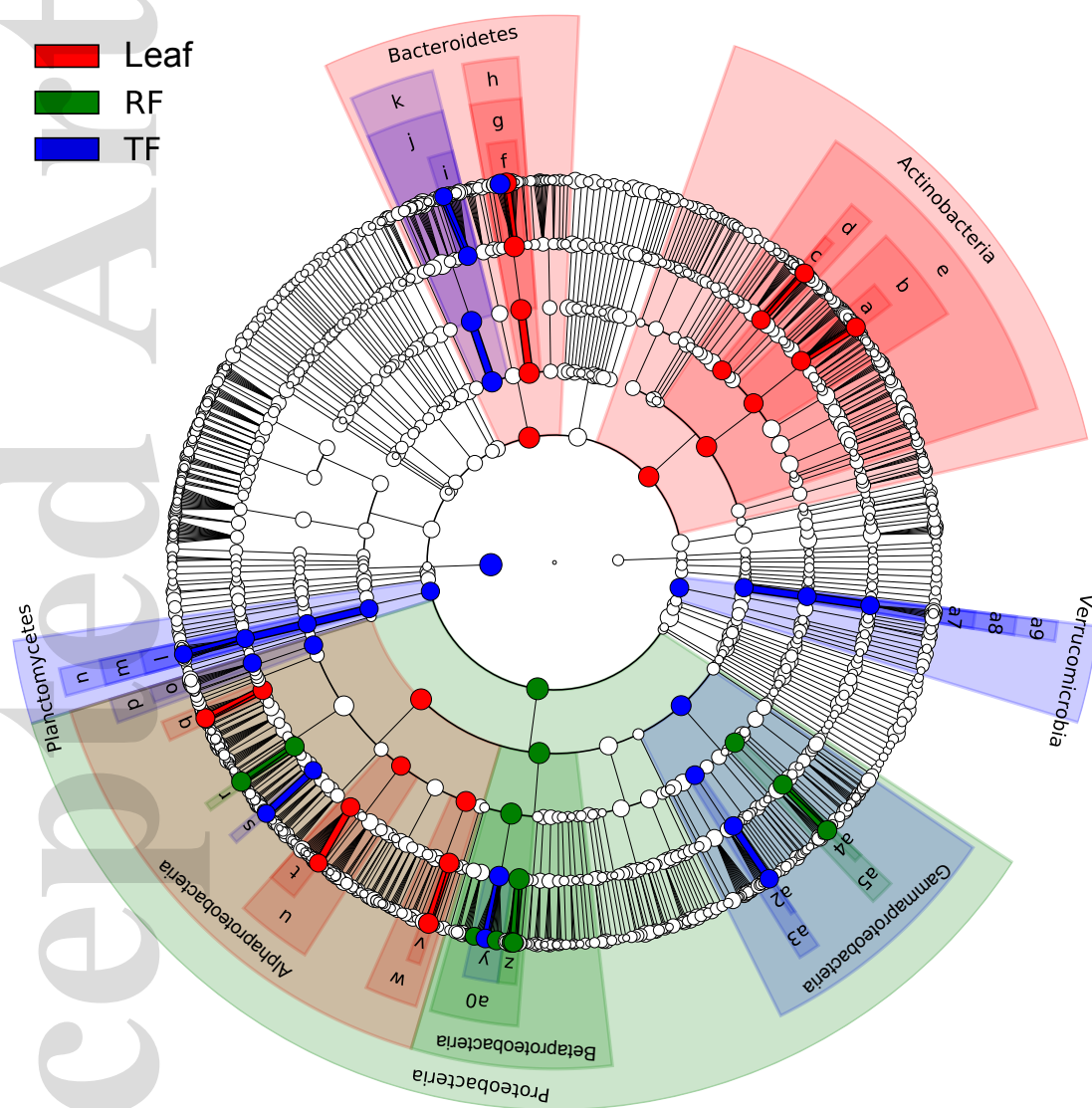| **Study site characteristics**		
Topographic characteristics		
	Altitude (m asl)	765
	Aspect	SW
	Distance to sea (km)	27
Climatic parameters [1]		
	Mean annual temperature (ºC)	9.0
	Mean annual precipitation (mm)	938
Stand parameters		
	Leaf area index (m^2 m^{-2})	6.1
	Number trees ha^{-1}	2571
	Mean diameter at breast height (cm)	13
	Basal area (m^2/ha)	26.5
	Age (year)	70
Air quality[2]	HNO_3 (μg m^{-3})	3.3
	NO_2 (μg m^{-3})	4.3
	NH_3 (μg m^{-3})	0.7
Wet N deposition[3]	NH_4-N (kg ha^{-1} $year^{-1}$)	2.61 ($\pm$0.79)
	NO_3-N (kg ha^{-1} $year^{-1}$)	2.79 ($\pm$0.53)

[1] Average 1984-2017

[2] Average 2011-2013 (García-Gómez et al., 2016)

[3] Average of N fluxes for hydrologic years 1983-84 to 2015-16 (n=33, 3 years without measurements).

Leaf
RF
TF

Bacteroidetes

Actinobacteria

Planctomycetes

Verrucomicrobia

Alphaproteobacteria

Gammaproteobacteria

Betaproteobacteria

Proteobacteria

Bacterial taxa

a: F_Microbacteriaceae
b: O_Micrococcales
c: F_Propionibacteriaceae
d: O_Propionibacteriales
e: C_Actinobacteria
f: F_Cytophagaceae
g: O_Cytophagales
h: C_Cytophagia
i: F_Chitinophagaceae
j: O_Sphingobacteriales
k: C_Sphingobacteriia
l: F_Planctomycetaceae
m: O_Planctomycetales
n: C_Planctomycetacia
o: F_Caulobacteraceae
p: O_Caulobacterales
q: F_1174_901_12
r: F_Methylobacteriaceae
s: F_Rhizobiales Incertae Sedis
t: F_Acetobacteraceae
u: O_Rhodospirillales
v: F_Sphingomonadaceae
w: O_Sphingomonadales
x: C_Alphaproteobacteria
y: F_Comamonadaceae
z: F_Oxalobacteraceae
a0: O_Burkholderiales
a1: C_Betaproteobacteria
a2: F_Legionellaceae
a3: O_Legionellales
a4: F_Pseudomonadaceae
a5: O_Pseudomonadales
a6: C_Gammaproteobacteria
a7: F_Verrucomicrobiaceae
a8: O_Verrucomicrobiales
a9: C_Verrucomicrobiae